

# PERFORMANCE OF VORTEX TURBINES IN ULTRA-LOW-HEAD HYDROELECTRIC POWER PLANTS: A NUMERICAL STUDY

Firdaus Ashar<sup>1)</sup>, M. Furkon Hakim<sup>2)</sup>, Sunaryo<sup>3\*)</sup>  
Universitas Sains Al-Qur'an, Indonesia

<sup>1)</sup> firdausasyhar@email.com, <sup>2)</sup> furkonhakim68@yahoo.com, <sup>3)</sup> sunaryo@unsiq.ac.id

\*sunaryo@unsiq.ac.id

**Submitted** :20 Oktober 2025 | **Accepted** : 29 Oktober 2025| **Published** : 31 Oktober 2025

**Abstract:** The performance of vortex turbines in ultra-low-head hydropower plants is crucial for harnessing energy in irrigation channels and small rivers. Therefore, an optimal design is needed to maximize the conversion of flow energy into electrical power. This study aims to evaluate and determine the best-performing configuration of ultra-low-head vortex turbines. The method used is Computational Fluid Dynamics (CFD) simulations employing the k- $\omega$  Standard turbulence model, with variations in the number of blades (3, 5, and 7) and a fixed blade angle of 15°. The results show that the 7-blade configuration with a 15° angle provides superior performance, generating 3.90 W of power, reducing NPSH by 2%, and increasing force by 6%, with a force value of 52.65 N. The implications of these findings suggest that the 7-blade–15° configuration is a suitable design reference for optimizing ultra-low-head vortex turbines in micro-scale hydroelectric power plants, supporting the utilization of renewable energy in irrigation networks and rural areas.

**Keywords:** Turbine vortex, CFD, Cavitation, Performance, Hydroelectric

## 1. INTRODUCTION

A turbine is a component that converts kinetic energy into mechanical energy, which drives a generator to produce electrical energy (Antono et al., 2016). In practice, turbines encounter technical or mechanical challenges, one of which is cavitation. Cavitation refers to the vaporization of a liquid forming bubbles, caused by insufficient fluid pressure in the water flow (Biantoro et al., 2016). Cavitation, derived from the Latin word "cavus," meaning empty, occurs when the pressure is too low, or in areas with low pressure or high velocity, cavitation is more likely to occur (Gurning et al., 2017).

A study on cavitation in the Francis turbine runner at the Batang Agam Hydroelectric Power Plant (PLTA) found that the cavitation coefficient is directly proportional to the water flow velocity. The highest cavitation coefficient was 0.111157 at a flow rate of 4.8 m<sup>3</sup>/s and 127.158 rpm, while the lowest coefficient was 0.106414 at a flow rate of 0.9 m<sup>3</sup>/s and 62.318 rpm (Putra et al., 2021). Research on the effect of blade opening on the cavitation level of the Francis horizontal turbine at the suction side of the Pakkat PLTA pipeline indicates that

cavitation begins to occur at blade openings between 10% and 18%. Cavitation decreases at blade openings between 40% and 69%, with the safe blade opening suggested at 69% (Sitompul et al., 2021). A numerical simulation on the effect of cavitation on the characteristics of the pump-turbine hump revealed a cavitation coefficient of 0.16. The total hydraulic loss increases sharply in the runner and stay/guide vane, with hydraulic losses in the runner rising from 28.3% ( $\sigma=0.16$ ) to 42.5% ( $\sigma=0.076$ ), while losses in the stay/guide vane decrease from 55.2% ( $\sigma=0.16$ ) to 48.8% ( $\sigma=0.076$ ) (Li et al., 2021). A numerical study on the cavitation effects on pressure fluctuations in the pump-turbine hump area found that cavitation generated a frequency of 1.344  $f_n$  (rational runner frequency) in the draft tube, originating from the oscillating flow at the outlet, and 2.88  $f_n$  in the runner caused by cavitation at the blade's suction surface. Additionally, cavitation at the stay and guide vanes increased pressure fluctuation amplitudes by 0.144  $f_n$  (Li et al., 2022).

Research on the development and application of the Entropy Production Diagnostic Model (EPDM) for cavitating pump-turbine flow in pump mode showed that the cavitation level decreased after a 3% head drop at  $\psi = 1.15$ , which is the closest distance between head drops of 3% and 4%. It then decreased to  $\psi=0.6$  and further reduced, ending at  $\psi = 0.8$ . The conclusion indicates that cavitation develops under overload conditions (Wang et al., 2020). A study on vortex rope formation and pressure fluctuations using anti-swirl fins in a Francis turbine model under partial load conditions, with the cavitation onset point approached using CFD, showed a velocity decrease with a fin set of 1 by 20.4% and 22%. The rotation intensity along paths 1 and 2 was 94% and 82%, respectively. The frequency pressure decreased by approximately 60% due to vortex rope formation with fin set 1 and set 2, while the frequency pressure decrease without fins was around 52% (Shahzer et al., 2022). The impact of cavitation and the influence of suction head on the Francis turbine, modeled using CFD CFX code, showed that cavitation occurred at  $\frac{H_s}{H} = 0.311$ . The maximum and minimum head loss difference was 2% with and without cavitation. Cavitation occurred when the tangential velocity increased by 25.8%, axial velocity decreased by 20.6%, and vortex strength increased by 77.8%. Safe turbine operation with suction head occurred between 0.135 and 0.311 (Shahzer et al., 2022).

Investigation of cavitation in a Francis turbine by varying rotational speed using a CFD approach revealed that the cavitation level was low initially ( $0.14 \leq n_{ED} \leq 0.20$ ), and during the subsequent phase ( $0.14 \leq n_{ED} \leq 0.20$ ), intense cavitation occurred throughout the turbine. The frequency increased from 206.7 Hz to 324.8 Hz between 1 and 6 seconds, with the highest cavitation effect occurring at 5.8 seconds (Trivedi et al., 2020). The impact of mass on the runner of the Francis turbine and cavitation in a single blade, analyzed using CFD, showed a cavitation value at a frequency of 228.3 Hz (46.6%) (Huang et al., 2019). A numerical study on the influence of cavitation on the axial force of the impeller blade in pump mode of a reversible pump-turbine, showed that the cavitation coefficient under partial load  $C_\phi = 0.0537$  decreased from 0.291 to 0.055. The amplitude variation was approximately 4.1% of the axial force under cavitation-free conditions. At design load  $C_\phi = 0.0672$ , cavitation decreased to 0.085, with amplitude variation around 1.9% of the axial force in cavitation-free conditions. Under overload conditions  $C_\phi = 0.0807$ , cavitation decreased to 0.219 (Zhu et al., 2021).

The potential for cavitation damage using the pulsation pressure phenomenon in low-head Francis turbines showed results with a plant discharge coefficient of 1.0 at measured load and 0.8 at full load. The discharge coefficient was 0.37 at lower load, and at  $1^{th}/5$  of the rotational frequency, observations yielded a frequency of 2.65 Hz, with a 36.81% amplitude increase observed under cavitation conditions. The maximum amplitude was found with a high discharge coefficient of 1.29 under overload conditions (Gohil et al., 2022). A study on the effect of anti-cavitation on the performance and vortex leakage characteristics of tubular turbines for marine power plants indicated that the leakage volume decreased by 13.28% under optimal conditions, and the maximum leakage volume decreased by 37.72% under off-design conditions (Li et al., 2023).

Previous studies have extensively investigated the phenomenon of cavitation in turbines, both through experimental and simulation methods, by varying several parameters such as the cavitation coefficient, flow rate, rotational speed, blade opening, suction head, and the application of anti-swirl fins, often utilizing Computational Fluid Dynamics (CFD) simulations with various turbulence models. These studies have provided valuable insights into the impact of cavitation on hydraulic losses, pressure fluctuations, axial forces, and turbine performance under various operating conditions (partial load, design load, and overload). However, there is no analytical or numerical study specifically focused on the impact of varying the number of blades (3, 5, and 7 blades) on the cavitation level in a turbine with a fixed blade angle of  $15^\circ$ , using CFD simulations with the  $k-\omega$  Standard turbulence model and the assumption of steady fluid flow. This gap constitutes the core problem to be investigated.

## 2. RESEARCH METHODS

The geometry of the ultra-low-head vortex turbine was designed using 3D software, considering the geometry from the literature (M. Safi'i et al., 2024). The geometry of the ultra-low-head vortex turbine consists of a basin and blades, with variations in the number of blades (3 blades, 5 blades, 7 blades) and a fixed blade angle of  $15^\circ$ .

### 2.2 Computational domain

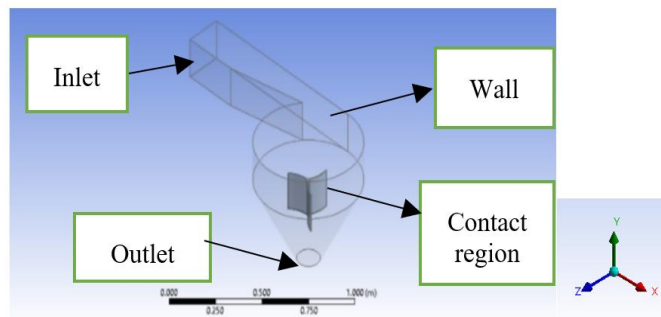


Figure 1. Computational Domain and Boundary Condition Determination in the Ultra-Low-Head Vortex Turbine.

A steady flow simulation was used to solve this simulation, although we assume the continued influence of gravitational forces that drive the water and external forces that arise, with potential energy being converted into kinetic energy. The computational domain, as shown in Figure 1, uses a Cartesian coordinate system, where the X-axis is the streamwise axis, the Y-axis is the transverse axis (spanwise), and the Z-axis is the normal axis to the XY plane (M. Safi'i et al., 2024). The average Reynolds number and the Navier-Stokes continuity equation were solved using the viscous  $k-\omega$  STD model, which can solve the numerical equations quickly, accurately, and precisely, depending on the assumptions of the selected viscous model (M. Safi'i et al., 2024).

In the simulation, the convergence criteria were set with energy residuals of  $10^{-3}$ , and for continuity, momentum, and  $k-\omega$ , the residuals were also  $10^{-3}$ . The viscous  $k-\omega$  STD model used in this numerical study assumes water at  $25^\circ\text{C}$  with material properties: density  $\rho = 998$  ( $\text{kg}/\text{m}^3$ ), specific heat  $C_p = 1.0057$  ( $\text{J}/\text{kg}^\circ\text{C}$ ), and viscosity  $\mu = 0.00001915$  ( $\text{N}/\text{s}/\text{m}^2$ ).

### 2.3 Meshing

In the numerical analysis, the governing equations were solved with the specified boundary conditions. The size and type of mesh significantly influence the accuracy and quality of the simulation results. The mesh type used is the Tetrahedral method, as this type of mesh can optimize the number of grids, which impacts the

reduction in computational cost (M. Safi'i et al., 2020). The mesh details used in this study are shown in Figure 2. A control-volume-based technique was employed to discretize the equations, using a first-order upwind scheme for higher accuracy with relatively fast numerical calculations. The computational domain was discretized with Tetrahedral mesh, fully structured with high resolution near the wall to capture the thermal boundary layer effects.

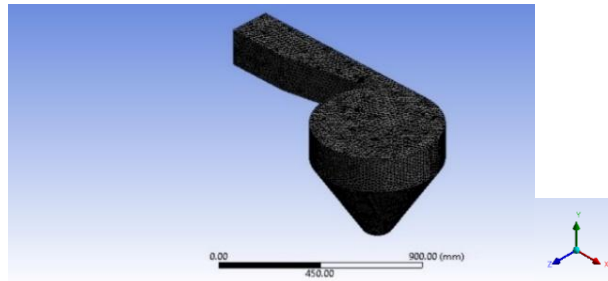


Figure 2. Meshing of the Ultra-Low-Head Vortex Turbine.

The mesh size is differentiated between the body sizing for the fluid and the body sizing for the geometry of the Basin and Runner being tested. The mesh size was set to 10 mm, with a total of 22,082 cells for the Runner geometry, while for the fluid, the total number of cells was 505,745. The mesh is considered to be of good quality if the Orthogonal Quality is between 0.95 - 1, the maximum skewness is between 0 and 0.25, and the wall  $y^+$  value is 1 (M. Safi'i et al., 2020).

#### 2.4 Grid Independence Test

A grid independence test was conducted to determine the optimal point for the experimental value, which is the average flow velocity in the vortex turbine. The grid test was performed by considering the number of mesh cells in the computational domain, with values of 215,830, 331,139, 446,177, and 523,388. The step-by-step simulation setup procedure was based on references from the literature.

The results of the grid test are presented in a graph showing the relationship between the grid number and the NPSH value against the number of grids in the Vortex Turbine, as illustrated in Figure 3. The calculations in the numerical study for the grid test indicate a relative error of  $\pm 3.7\%$  between grid 215,830 and 331,139,  $\pm 2.4\%$  between 331,139 and 446,177, and  $\pm 2.2\%$  between 446,177 and 523,388. The optimum mesh for the numerical study was marked by a skewness mesh metric spectrum value of 0.2 and an orthogonal quality mesh metric spectrum value of 0.8. This was further validated by the standards set by software simulation for mesh quality.

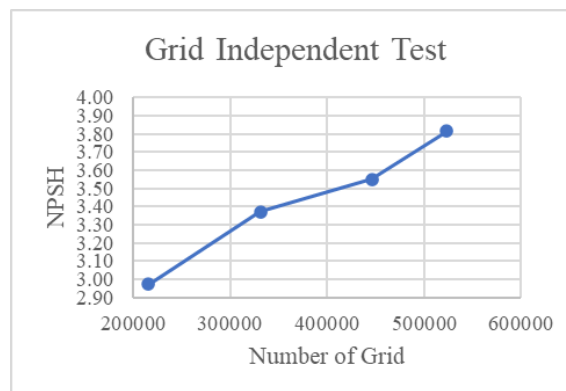


Figure 3. NPSH Value vs. Grid Number in the Vortex Turbine.

## 2.5 Validation

Validation was performed to ensure that the CFD simulation methods and results are accurate. There are two validation processes: convergence and grid testing. Convergence refers to the solver control equation settings aimed at minimizing simulation errors. The calculations or iteration process in the flow solver phase are carried out once all boundary conditions are defined. The number of iterations is influenced by the accuracy of the model created. If a higher number of grids is used in the modeling, the iterations will increase. The iteration process will stop once the convergence limit is reached. This calculation process continues until the smallest error or convergent value is obtained (M. Safi'i et al., 2022).

Validation was carried out through a numerical approach to the experiments conducted in the literature (M. Safi'i et al., 2024). The parameter of interest in this study is the NPSH coefficient of the vortex turbine. Validation was done with variations in simulation methods at a mesh cell count of 523,388. The validation results are shown in Figure 4, illustrating the variation of simulation methods against NPSH. Only the best results are presented in this report. The graph shows that the experiment conducted in the literature (M. Safi'i et al., 2024) for the vortex turbine yielded an NPSH value of 3.708 using the coupled method. The comparison between the simulation results and the literature experiment shows a relative error of 1% in the NPSH value. Figure 4 also demonstrates that the NPSH value increases as the Reynolds number increases. However, it is strange that at a Reynolds number of 12,051.964, the NPSH value decreases.

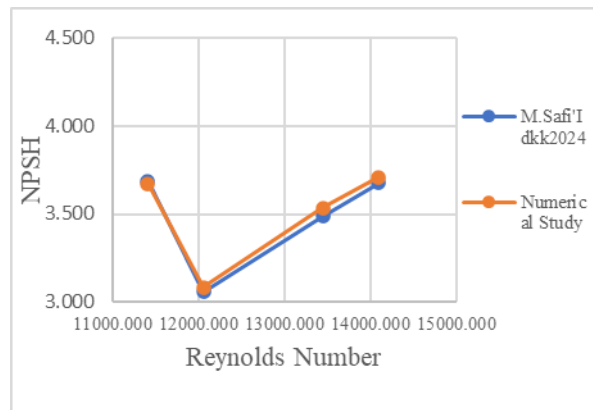


Figure 4. Reynolds Number vs. NPSH in the Vortex Turbine.

## 2.6 Numerical Data Reduction

The process of modeling the pump turbine involves determining the values for calculations. By referencing the calculation values, an optimal turbine design can be achieved.

### a. Viscosity

$$\mu = \frac{\nu}{\rho}$$

Kinematic viscosity is obtained based on the correlation between dynamic viscosity divided by the density of water.

### b. Prandtl Number

$$Pr = \frac{\mu \cdot Cp}{k}$$

The Prandtl number is a dimensionless number that represents the relationship between kinematic viscosity and thermal diffusivity.

c. Potential Energy

Potential energy per unit time or potential power ( $P_p$ ). To calculate the potential energy available in a vortex cone basin, the gravitational potential energy of the water flowing through the system must be considered (M. Safi'i et al., 2024).

$$P_p = \rho \cdot Q \cdot g \cdot h$$

d. Power

To calculate the theoretical power that can be generated by the vortex cone basin (M. Safi'i et al., 2024).

$$P = \eta \cdot \rho \cdot Q \cdot g \cdot h$$

e. Motor power

Motor power is the required value for the turbine to handle the pumped fluid.

$$P_t = Q \cdot g \cdot h$$

f. Basin volume

The basin volume is the measure of the amount of substance entering the turbine basin.

$$V = \frac{1}{2} \cdot \pi \cdot r^2 \cdot h$$

g. Cross-sectional Area

The cross-sectional area, in this case, refers to the inlet channel of the basin. To calculate the cross-sectional area of the vortex cone inlet channel, the trapezoidal area formula can be used (M. Safi'i et al., 2024).

$$A = \frac{1}{2} \cdot (a + b) \cdot h$$

h. Mechanical Energy

The mechanical energy generated by the turbine is the energy conversion of kinetic energy into mechanical energy. The turbine operates by passing fluid flow (gas or liquid) through stationary and moving blades.

$$P = C_p \cdot \frac{1}{2} \cdot \rho \cdot A \cdot V^3$$

i. Efficiency

Efficiency is the ratio between the volume of fluid and volume, while in pump turbines, it refers to the displacement of fluid with a liquid according to its volume (Dewadi et al., 2023).

$$\eta = \frac{P}{P_t} \times 100\%$$

### 3. RESULTS AND DISCUSSION

Cavitation in the vortex turbine was investigated numerically and experimentally using a CFD simulation approach. Several variations were considered, such as the number of blades (3 blades, 5 blades, and 7 blades), with a blade angle of 15°.

#### 3.1 Effect of blade number on cavitation

The vortex turbine is classified as a reaction turbine, which is used in rivers or water flows with very low heads (Susanto et al., 2024). The vortex turbine is also categorized as an axial turbine because the fluid flow operates parallel to the shaft (M. Safi'i et al., 2024). The working principle of the vortex turbine begins with the water fluid being directed to the circulation tank. Inside the volute, the strength of the vortex flow is influenced by the low pressure and the water velocity at the inlet point of the tank, where potential energy is then converted into kinetic energy. The water fluid is then discharged back into the river through the outlet channel (Rinanda and Permatasari, 2018).

A numerical study in this research was conducted to understand and predict the effect of blade number on the performance of the ultra-low-head vortex turbine. It is expected that this research will provide performance data for the vortex turbine that can be practically applied in the field, considering the high demand for electrical energy by the community to support household activities and lighting. The number of blades proposed is 3, 5, and 7, which are characterized to find the most optimal performance data and design for the ultra-low-head vortex turbine.

The flow characteristics in the vortex turbine initially form a stable flow as the water fluid enters the basin geometry. The presence of blades causes flow separation and pressure differences, which result in drag forces around the runner. As a result, the flow becomes unstable, leading to flow turbulence in the vortex turbine. Additionally, vortex waves or vortices occur due to linear momentum in the form of hydrostatic forces acting on the helical blades, causing centrifugal forces to work at higher levels.

Figure 5 shows the characteristics of the velocity streamline contour in the vortex turbine. The figure illustrates that the flow velocity in the vortex turbine is uneven, with the maximum average flow velocity occurring in the range of 32.13 m/s to 42.82 m/s.

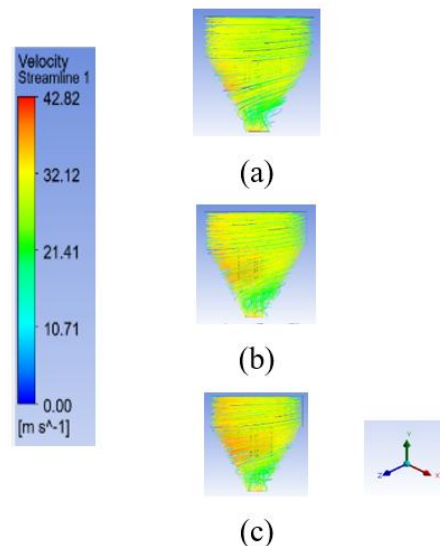


Figure 5. Velocity Distribution Contours in the Vortex Turbine Basin, (a) 3-Blade, 15° Angle, (b) 5-Blade, 15° Angle, (c) 7-Blade, 15° Angle.

### 3.2 Effect of Basin

Several factors can influence the flow velocity in this turbine, such as the basin slope, basin roughness, and the size and shape of the basin. Changes in the flow velocity of the fluid in the turbine are generally caused by frictional forces between fluid particles, friction between the fluid particles and the basin walls, and collisions of fluid particles with the blade walls (M. Safi'i et al., 2024). Figure 6 shows the relationship between the number of blades and blade angle on the force in the vortex turbine. The results of the numerical study indicate that the force value for the 7-blade variation has the best force value at 52.65 N.

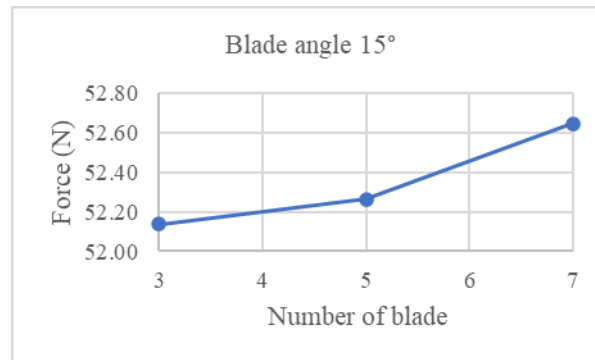


Figure 6. Graph of the Effect of Blade Number on Force (N).

The increase in the number of blades in this numerical study is expected to enhance the force value in the ultra-low-head vortex turbine. It has been proven to increase the force value by 6%, improving the turbine performance. Furthermore, the NPSH value becomes smaller, suggesting that increasing the number of blades may further increase the force value and reduce the NPSH. The force value in the ultra-low-head vortex turbine plays a crucial role in the turbine's performance. It is known that the force value provides significant thrust on the turbine runner, allowing for a large centrifugal force effect, which results in faster turbine rotation.

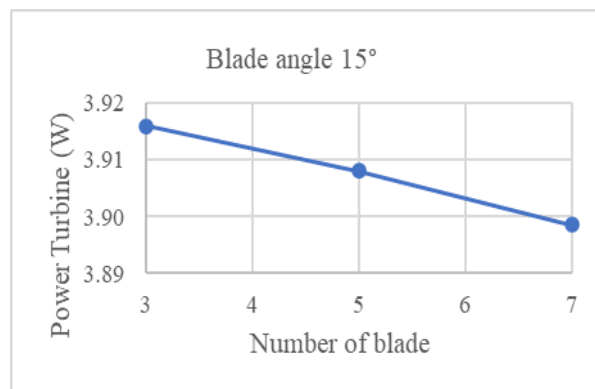


Figure 7. Graph of the Effect of Blade Number on Turbine Power (W)

The graph shown in Figure 7 illustrates that as the blade angle increases and the number of blades increases, the power output of the vortex turbine decreases. With 7 blades and a 15° blade angle, the turbine is able to generate a power output of 3.90 W. The phenomenon observed is that the water fluid entering through the basin inlet generates significant centrifugal force, causing the blade rotation to increase, which in turn allows the turbine power to rise. The increase in turbine power results in higher electrical energy production. Furthermore, with the increased turbine power, the turbine operates more efficiently.

The turbine power generated from the proposed turbine design in this research is derived from the conversion of fluid energy into work. The cavitation phenomenon in this numerical study occurs when air bubbles form around the blades and slowly collapse due to pressure loss. This cavitation phenomenon can lead to damage to the runner and basin. If left unaddressed, cavitation may cause flow losses (head loss), which significantly affect the turbine's flow conditions. Weak flow conditions lead to insufficient torque and turbine power. Increasing the number of blades can reduce the NPSH value by 2%. The turbine power values for 3 blades are 3.92 W, for 5 blades are 3.91 W, and for 7 blades are 3.90 W.

#### 4. CONCLUSIONS



Based on the research results, cavitation analyzed both experimentally and numerically can be concluded as follows. The cavitation conditions caused by the effects of blade number and blade angle show that the performance characteristics do not change when the cavitation coefficient is greater than 0.16. When the cavitation coefficient is between 0.075 and 0.16, the performance characteristics decrease due to the reduction in cavitation. When the cavitation coefficient is less than 0.075, the performance characteristics sharply decline as the cavitation coefficient decreases. The increase in force by 6% improves the turbine's performance. With 7 blades, the force value reaches 52.65 N. This increase in force leads to a lower NPSH value, which in turn reduces cavitation. Additionally, the increase in the number of blades has been shown to reduce cavitation, with the NPSH value decreasing by 2%. The optimal number of blades in this study is 7, based on the power output value of 3.90.

This research has direct implications for turbine design optimization. By determining the optimal number of blades (3, 5, or 7) that minimizes cavitation at a fixed 15° angle, the findings will provide crucial design guidelines to reduce cavitation damage, extend turbine life, and enhance overall hydraulic efficiency in hydropower operations.

## 5. REFERENCE

- Antono, V. & Yusreza, C. F. A. R., 2016, "Perancangan PLTMH Kapasitas 30 kW, Desa Giritirta, Kec. Pejawaran, Banjarnegara, Jawa Tengah", *Jurnal Power Plant*, Vol. 4, hlm 107-13.
- Biantoro, T. & Siswanto, S., 2016, *Analisa Kavitasasi Yang Terjadi Pada Turbin Francis di PLTA PB Soedirman, Laporan Penelitian, Universitas Gajah Mada, Yogyakarta.*
- Gohil, P. P. & R.P. Saini, R. P., 2022, "Investigation into cavitation damage potentiality using pressure pulsation phenomena in a low head Francis turbine for small hydropower schemes", *Journal Ocean Engineering*, Vol 263, hlm 112-230.
- Gurning, F. P., Nasution, A. H., Gultom, S., Lubis, Z. & Ariani, F., 2017, "Pengaruh Bukaan Sudu Pengaruh Terhadap Tingkat Kavitasasi Di Sisi Masuk Pipa Isap Turbin Francis Vertikal", *Jurnal Dinamis*, Vol. 5, hlm 24-36.
- Huang, X. & Escaler, X., 2019, "Added Mass Effect on Francis Turbine Runner with Attached Blade Cavitation", *Jurnal Fluids*, Vol 4, hal 107.
- Li, C., Luo, X., Wu, G., Fu, Y., Feng, J. & Zhu, G., 2023, "Investigation on effect of anti-cavitation edge on performance and leakage vortex characteristics of tubular turbine for ocean power generation", *Journal Ocean Engineering*, Vol 281, hlm 114-797.
- Li, D., Song, Y., Lin, S., Wang, H., Qin, Y. & Wei, X., 2021, "Effect mechanism of cavitation on the hump characteristic of a pump-turbine", *Jurnal Renewable Energy*, Vol 167 hlm 369-383.
- Li, D., Song, Y., Lin, S., Wang, H., Qin, Y. & Wei, X., 2022, "Cavitation effects on pressure fluctuation in pump-turbine hump region", *Journal of Energy Storage*, Vol 47 hlm 103-936.
- Putra, R. H., Arif, R. K. & Muchlisinalahuddin., 2021, "Analisis Tingkat Kavitasasi Turbin Francis di PLTA Batang Agam", *Jurnal Terapan Teknik Mesin*, Vol. 2, hlm 78-87.
- Rinanda, Vico. & Permatasari, Rosyida., 2018 "Optimasi Desain Turbin Air Tipe Vortex Dengan 5 Variasi Jumlah Sudu Terhadap Efisiensi", *Seminar Nasional Cendekiawan ke 4 Tahun 2018.*
- Safi'I, M., Sinaga, N. & Amin, M. S, 2024, "Investigasi Model Numerik Turbin Reaksi Vortex Ultra Low Head Dengan Memvariasikan Jumlah Grid Dan Metode Pemecahan Solusi", *Jurnal Device*, Vol. 14, hlm 225-235.
- Shahzer, M. A., Kim, S. J., Cho, Y., Choo, S. N., Nam, H. W. & Kim, J. H, 2022, "Effect of Suction Head on Inception and Development of Cavitation in a Francis Turbine Model", *Journal of Fluid Machinery*, hlm 13-22.
- Shahzer, M. A., Kim, S. J., YongCho, Y. & Kim, J. H., 2022, "Suppression of vortex rope formation and pressure fluctuation using anti-swirl fins in a Francis turbine model at part load condition with cavitation inception point", *Jurnal Physics of Fluids.*



Clean Energy and Smart Technology

## Clean Energy and Smart Technology

Volume 04, Number 01, October 2025

DOI : <https://doi.org/10.58641/cest.v4i1.171>

e-ISSN : 2964-2647

- Sitompul, Y. S., Rahmawati. & Ibrahim, H., 2021, "Analisis Pengaruh Bukaannya Sudu Terhadap Tingkat Kavitasinya Di Sisi Masuk Suction Pipe Turbin Francis Horizontal Unit 3 di PLTA Pakkat PT Energy Sakti Sentosa", jurnal Konferensi Nasional Sosial dan Engineering Politeknik, hlm 216-221.
- Trivedi, C., Iliev, I., Dahlhaug, O. G., Markov, Z., Engstrom, F. & Lysaker, H., 2020, "Investigation of a Francis turbine during speed variation: Inception of cavitation", Jurnal Renewable Energy, Vol 166, hal 147-162.
- Wang, C., Zhang, Y., Yuan, Z. & Ji, K., 2020, "Development and application of the entropy production diagnostic model to the cavitation flow of a pump-turbine in pump mode", Journal Renewable Energy, Vol 154, hlm 774-785.
- Zhu, D., Xiao, R. & Liu, W., 2021, "Influence of leading-edge cavitation on impeller blade axial force in the pump mode of reversible pump-turbine", Journal Renewable Energy, Vol 163, hlm 939-949.



This is an Creative Commons License This work is licensed under a Creative Commons Attribution-NonCommercial 4.0 International License.